# Sum rules for quasifree scattering of hadrons

R. J. Peterson*
*Department of Physics, University of Colorado Boulder, Boulder, Colorado 80302-0390, USA*

(Received 1 August 2017; published 12 February 2018)

The areas $d\sigma/d\Omega$ of fitted quasifree scattering peaks from bound nucleons for continuum hadron-nucleus spectra measuring $d^2\sigma/d\Omega d\omega$ are converted to sum rules akin to the Coulomb sums familiar from continuum electron scattering spectra from nuclear charge. Hadronic spectra with or without charge exchange of the beam are considered. These sums are compared to the simple expectations of a nonrelativistic Fermi gas, including a Pauli blocking factor. For scattering without charge exchange, the hadronic sums are below this expectation, as also observed with Coulomb sums. For charge exchange spectra, the sums are near or above the simple expectation, with larger uncertainties. The strong role of hadron-nucleon in-medium total cross sections is noted from use of the Glauber model.

DOI: 10.1103/PhysRevC.97.024609

## I. INTRODUCTION

Chemists tell us with certainty the charge held within an atomic nucleus, but whether this charge is held only in the integral number of protons in that nucleus can only be determined by some counting system. The scattering of electrons from nuclear charge can do this counting, under the assumptions of the quasifree scattering approximation. These conditions are found in Ref. [1] and are readily met by electron beams of several hundred MeV. The Rosenbluth decomposition [2] allows researchers to separate the scattering of electrons from nuclear or nucleon charge from magnetic scattering. This allows direct counting of the protons within a nucleus.

It is a feature of quasifree scattering that scattering cross sections are added incoherently, in contrast to coherent scattering where amplitudes are added [1]. Incoherent scattering from nucleons within a nucleus can be noted by the energy loss of the beam, with the recoil energy being that of a single bound nucleon. This energy loss can be much greater than that for coherent elastic scattering from the entire nucleus, which recoils with much lower energy. Many such electron spectra have been obtained, where the process is often called "quasielastic," not quasifree. Reference [1] clearly distinguishes between these very different usages in Chapter 11.

If the doubly-differential cross sections $d^2\sigma/d\omega d\Omega$ for quasifree charge scattering of electrons are integrated across the outgoing energies, the area $d\sigma/d\Omega$ normalized to free charge scattering and to the charge of the target should be unity, as if the number of protons were the same as the nuclear charge $Z$. Several recent examples of these charge sum rules have been published [3–7], and their results are used in the figures below.

Beams of hadrons may also meet the conditions of Ref. [1] for quasifree scattering, but with several complications. Hadronic cross sections are large, and a beam particle may scatter from two or more nucleons, in contrast to rare scattering of electrons. One needs a system to count the number of one-and-only-one scattering events. These large cross sections also limit hadronic quasifree scattering to the lower densities of the nuclear surface. But hadronic interactions with bound nucleons are also more interesting than the electromagnetic interactions of electron beams, due to the strongly interacting environment around the beam-nucleon scattering. The hadron beam, the bound nucleon, and the interaction between them may all be influenced by the strong field. The simplest test of the assumptions and parameters for quasifree hadron scattering is the same sum rule as used for the charge scattering of electrons. This is the point of this work: using quasifree hadron spectra both with (SCX) and without (NCX) single charge exchange of the beam particle.

Figure 1 shows measured spectra for inclusive scattering without charge exchange (NCX) of 820 MeV pions from carbon [8], as an example of the data to be considered in this work. Coherent elastic and inelastic scattering at small energy loss drops quickly with increasing momentum transfer $q$, while the wide quasifree peak remains strong. Asymmetric Gaussian peaks fitted to these spectra above a linear background are also shown in Fig. 1 [8]. It is the areas of such quasifree peaks which are integrated to form the hadron quasifree sums in this work.

## II. METHODS

For incoherent quasifree scattering, the measured inclusive (single-arm) cross sections factor as

$$d^2\sigma/d\omega\, d\Omega = A_{\rm eff}\, d\sigma/d\Omega\, R\, K, \tag{1}$$

with $A_{\rm eff}$ the number of one-and-only-one hadron-nucleon collisions, $d\sigma/d\Omega$ the free-space hadron-nucleon cross section, and $R$ the single nucleon response. A kinematic factor $K$ is determined by the defined response. A test of the quasifree assumptions is found in the concept of scaling, whereby the

*jerry.peterson@colorado.edu

 

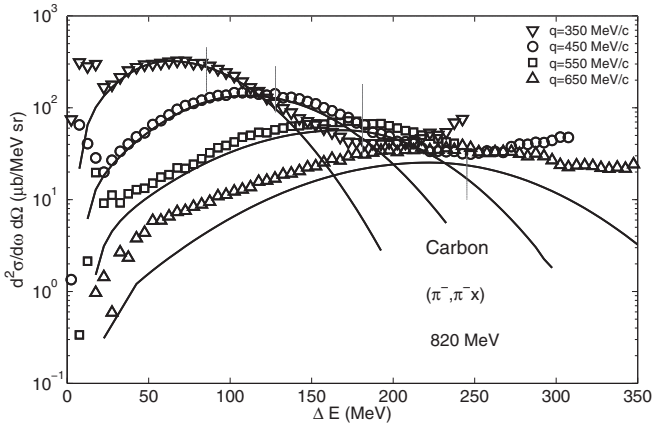


FIG. 1. Inclusive pion scattering spectra for carbon [8] are shown, together with fitted lines above an assumed linear background. Short vertical lines indicate the simplest energy losses for quasifree scattering, $q^2/2M + 20$ MeV (for binding, as Ref. [14]), with $M$ the free nucleon mass. The areas of the quasifree peaks are 27(3), 14.3(3), 7.75(1.6), and 4.06(2) mb/sr at $q = 350$, 450, 550, and 650 MeV/$c$. These singly-differential cross sections were used to compute the experimental sum rules.

momentum transfer $q$ and the energy transfer $\omega$ from the beam to the one struck nucleon are combined into a single variable. These scaling methods have been used for beams of electrons [9] and hadrons [10–12] and generally justify the factorization implied in Eq. (1).

In particular, quasifree electron scattering from bound protons has been used to form Coulomb sums, which could be expected to match the nuclear charge $Z$. In the present work, similar methods are used to create sums of nucleons $A$ for hadronic spectra without charge exchange, of protons $Z$ for hadronic charge exchange of negative pions, and of neutrons $N$ for charge exchange with proton beams.

The hadron spectra are not readily separated into their spin and isospin components, as there is no general Rosenbluth decomposition. The full areas under the quasifree (QF) peaks are used for hadronic sums, from fits such as the curves in Fig. 1. It is the areas $d\sigma/d\Omega|_{\rm QF}$ under these fit curves which are used to form the hadronic sum rules.

These integrated areas for the quasifree peak are converted to sum rules by

$$\text{Sum} = d\sigma/d\Omega|_{\rm QF} \times \text{PBF}/(d\sigma/d\Omega|_{\rm free} A_{\rm eff}), \qquad (2)$$

including the Pauli blocking factor (PBF) for momentum transfers less than $2k_{\rm F}$ [13]:

$$\text{PBF} = 3q/4k_{\rm F} - q^3/16k_{\rm F}^3 \qquad (3)$$

with Fermi momenta $k_{\rm F}$ from Ref. [14] and free-space differential cross sections $d\sigma/d\Omega|_{\rm free}$ [15]. Although the areas of the cross sections are unaffected by relativistic considerations, the Pauli blocking factor will be altered with relativistic kinematics. The relativistic Fermi gas responses [16] extend to lower energy losses than do the nonrelativistic curves, and face stronger blocking.

There remains the need to compute the number of nucleons the beam particle can see once and only once. This is computed in the Glauber model [17], as used for intermediate energy hadron quasifree reactions [18]. Integrals along $z$ across the nucleus for impact parameters $b$ are

$$A_{\rm eff} = 2\pi \int T(b) e^{-\text{SGT}\, T(b)}\, b\, db \qquad (4)$$

with the profile function

$$T(b) = \int \rho(r)\, dz. \qquad (5)$$

These integrals use the distribution of neutrons and protons with the same geometrical parameters [19] and the beam-nucleon total cross sections (SGT) [15]. Technical considerations for scatterings within nuclear matter decrease the measured total cross sections of Ref. [15], by a factor of 70% in Refs. [20–22], largely because the Pauli principle bars scattering into states already filled by nucleon momentum states.

At the higher beam energies of the data considered in this work, the in-medium total cross sections SGT are expected to be near those in free space [23]. Use of the full free-space SGT values in these integrals would lead to larger sum rules, typically by about 45% for carbon and 65% for lead. This work uses the 70% factor for free-space SGT to maintain consistency with earlier work on hadron quasifreee scattering.

Not all intermediate energy quasifree hadron spectra considered in this work were integrated by the author for the singly-differential cross sections needed for sum rules. Tables or figures of all these data were fit anew, using a planimeter for the smooth shapes above several estimated backgrounds of nonquasifree processes. Uncertainties reflect the choices for such backgrounds, with larger uncertainties at larger angles or momentum transfers.

The machinery needed to transform spectra as seen in Fig. 1 to hadronic sum rules is now complete.

## III. NCX SUM RULES

Figure 2 shows these NCX sums as measured for $^6$Li, compared to the PBF curve computed from $k_{\rm F} = 165$ MeV/$c$ [14]. No Coulomb sums are available for $^6$Li, but hadron data from proton [24] and pion [8] scattering are shown. A single data point is available from Ref. [25]. Except for this datum, the sums are very nearly as expected beyond the region of Pauli blocking. In these and other figures, open points denote data with negative beams, and solid points denote data with positive beams.

Similar data in Fig. 3 for carbon samples include the Coulomb sums (labeled as EEL), without theoretical tails, as reported in Refs. [4,5,7,26] and sparse $K^+$ data from Ref. [27]. Pion NCX data at 500 MeV are from Refs. [13,28]. Pion NCX data at 820 MeV are from Ref. [8]. Proton NCX data are shown at 392 [29], 400 [30], 795 [24], and 1014 MeV [31]. The Coulomb sums are about 80% of the expected value, while the 820 MeV pion data nearly match the expectation. The proton data are more scattered, and the $K^+$ data are again consistent, with a large uncertainty at the lowest of three $q$ points. Save for

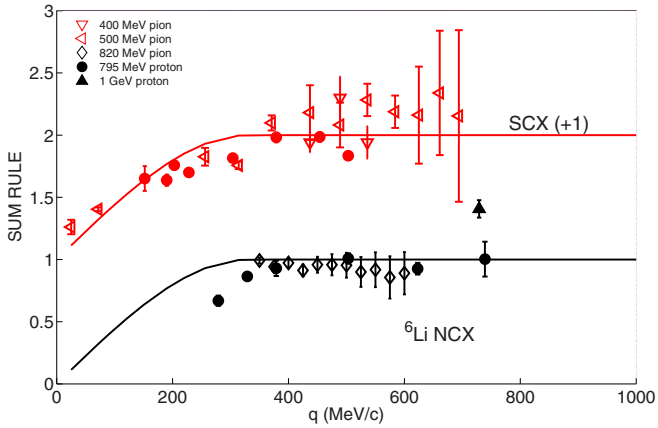


FIG. 2. Bottom: Measured areas of hadronic quasifree scattering peaks without charge exchange (NCX) on $^6$Li from Refs. [8,24], presented as sum rules as the momentum transfer $q$ to the struck nucleon increases. Top: Single charge exchange (SCX) areas (in red) on natural lithium from Refs. [37,43,44], as sum rules. Curves show the expected sums for a Fermi gas, including the Pauli blocking factor in the text, with $k_F = 165\,\mathrm{MeV}/c$.

the 1014 MeV proton data [31] read from a figure, the hadron data are consistent among themselves and nearly agree with the charge electron scattering sums. The Pauli blocking curves shown are computed for $k_F = 228\,\mathrm{MeV}/c$ [14]. The dashed theory curves [26] are discussed below.

NCX sum rules for aluminum are shown in Fig. 4. Proton data at 392 MeV are from Ref. [29] and data at 795 MeV are from Ref. [24]. The Pauli blocking curves use $k_F = 236\,\mathrm{MeV}/c$ [14].

For calcium in Fig. 5, the Coulomb sums [4,6,7] are about 60% of the expected value, while the 500 MeV NCX pion [13,28], 820 MeV pion [8], 367 MeV $K^+$ [27], 392 MeV [32], 420 MeV [33], 500 MeV [34], 795 MeV [24], 1014 MeV [31], and 1 GeV [35] proton data are much closer to the Fermi gas

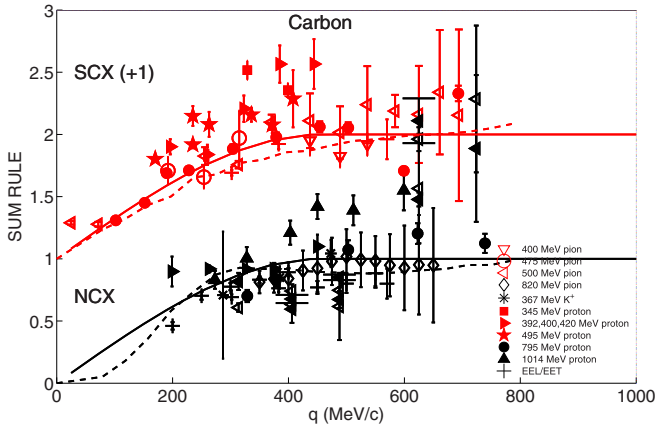


FIG. 3. As Fig. 2, but for a carbon sample, with $k_F = 228\,\mathrm{MeV}/c$. Data sources are presented in the text. Dashed curves show the one-body calculations for charge (bottom) and magnetic (top) electron scattering [26]. The charge electron scattering (EEL) sums among the NCX points and the transverse (EET) sums among the SCX points are from Ref. [26], with no tails added.

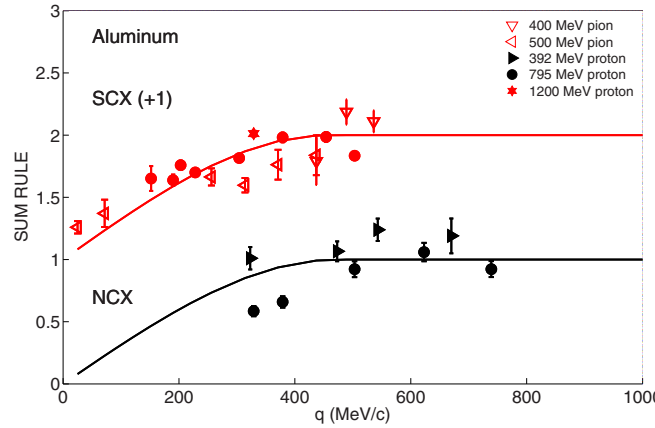


FIG. 4. As Fig. 2, but for an aluminum sample, with $k_F = 236\,\mathrm{MeV}/c$. Data sources are presented in the text.

expectation, which uses $k_F = 241\,\mathrm{MeV}/c$ [14]. Coulomb sums from electron scattering on an iron ($A = 56$) sample average 0.78(0.10) from the table of Ref. [7]. The pion NCX sums are below the expectation, and the charge sums yet further below.

For zirconium in Fig. 6, the 500 MeV NCX pion data are from Refs. [13,28] and data at 820 MeV are from Ref. [8]. $K^+$ data are from Ref. [27], 392 MeV proton data (on niobium) are from Ref. [29], and 795 MeV proton data are from Ref. [24]. The Pauli blocking curves use $k_F = 245\,\mathrm{MeV}/c$ [14].

For lead in Fig. 7, the 500 MeV NCX pion data are from Refs. [13,28] and the 820 MeV data are from Ref. [8]. The proton data are at 392 MeV [36], 500 MeV [34], and 795 MeV [24]. The Pauli blocking curves use $k_F = 248\,\mathrm{MeV}/c$ [14].

The three hadron probes span the possibilities of possible hadronic effects. The pion beams are akin to the main source of the nucleon mean field and of the interactions among bound nucleons. The proton beams are equivalent to the bound nucleons, with larger total cross sections than found for the pions. The $K^+$ beams have small total cross sections and the deepest access to the nuclear interior, while the electron beam sums scan the entire nuclear volume.

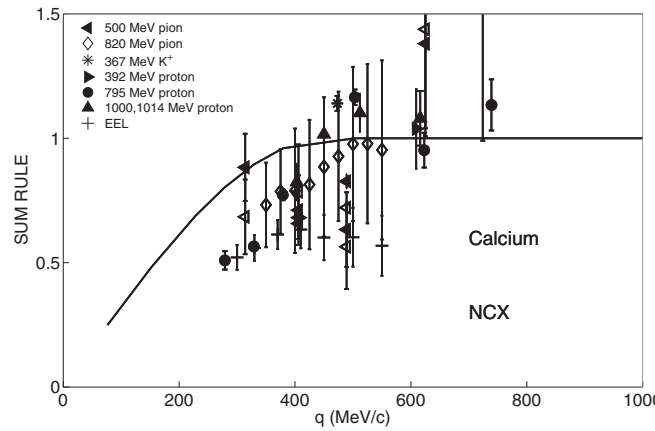


FIG. 5. As Fig. 2, but for a calcium sample with NCX hadron quasifree sums, with $k_F = 241\,\mathrm{MeV}/c$. Data sources are presented in the text.

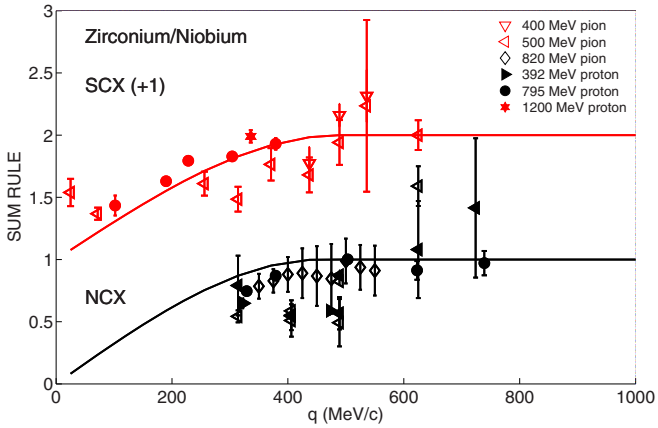


FIG. 6. As Fig. [2], but for zirconium and niobium samples, with $k_F = 245\,\mathrm{MeV}/c$. Data sources are presented in the text.

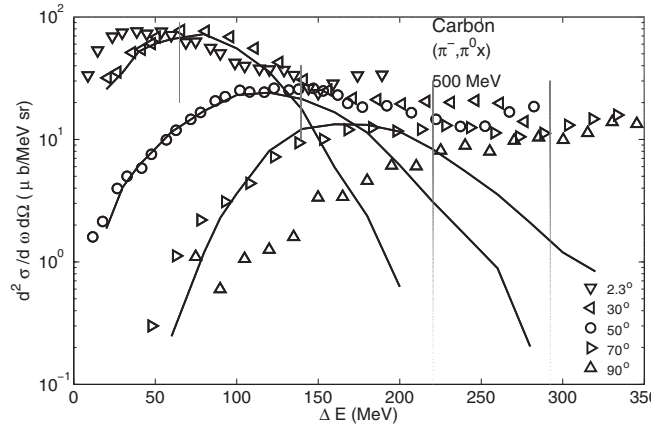


FIG. 8. The $(\pi^-, \pi^0 x)$ data for carbon of Ref. [37] are shown, as are fits above an assumed quadratic background (as curves). Vertical lines indicate the loci of free scattering $(q^2/2M) + 12.17$ MeV for binding [14], Coulomb, and $Q$-value effects.

These hadron beams do not sample the entire nuclear volume, as is the case with electron beams. For instance, the 820 MeV negative pions scatter once and only once for only $A_{\mathrm{eff}} = 3.805$ out of 12 in carbon and 15.21 out of 208 in lead, as reached by integration of the nuclear volume outwards from 2.47 fm for carbon and 7.38 fm for lead. The sum rules shown represent scattering only from nucleons at low densities.

## IV. SCX SUM RULES

Figure 8 shows typical quasifree SCX spectra from Ref. [37] with fits to allow integration for the singly-differential cross section $d\sigma/d\Omega$ to form sums as above. Fits shown as solid curves were for an asymmetric Gaussian quasifree peak atop a quadratic polynomial background at angles of 30°, 50°, and 70°. Vertical lines denote locations of the quasifree maxima expected for the last four angles, at momentum transfers ranging from 314 to 625 MeV/$c$. The quasifree SCX peak is nearly lost in the background at 90°.

Charge exchange experiments were carried out for 400, 475, and 500 MeV negative pions [37], and 345 [38–40], 392 [30], 495 [41–43], 795 [43,44], and 1200 MeV [45] protons. The $\pi^-$ SCX data were normalized directly to SCX on free protons and count protons, much as for the Coulomb sums. An indirect method was used to normalize $(p,nx)$ spectra, resulting in a change by a factor of 1.6 between Refs. [44] and [43] at 795 MeV.

Hadronic charge exchange reactions include $(\pi^-,\pi^0 x)$ inclusive charge exchange on protons and $(p,nx)$ charge exchange on neutrons. Sum rules divide cross sections by the elementary hadron-nucleon charge exchange cross sections [15]. For $(p,n)$ SCX reactions these are computed from the amplitudes within Ref. [15] by the formalism of Ref. [46]. SCX spectra for $\pi^-$ were calibrated and normalized directly to SCX measurements on free protons [37] and use SCX free cross sections from Ref. [15]. The sum rules are normalized to $Z_{\mathrm{eff}}$ or $N_{\mathrm{eff}}$, computed as fractions of computed $A_{\mathrm{eff}}$ by $Z/A$ or $N/A$.

Figure 2 shows SCX sums on natural lithium. Pion data are from Ref. [37], with 795 MeV proton data from Ref. [44]. These sums are nearly as expected, as was also the case with the more accurate NCX measurements.

SCX sums for carbon are shown in Fig. 3. The inclusive data for pion SCX are from Ref. [37] at three beam energies, while the 795 MeV proton data of Ref. [44] have been renormalized by a factor of 1.6. The 346 [38], 392 [30], and 495 MeV [41,42] data scatter about the expected curve. The transverse electron scattering sums, without added tails, from Ref. [26] are shown with these carbon SCX sums labeled as EET points.

Figure 4 shows sum rules extracted from SCX spectra on aluminum. The 500 MeV pion data are from Ref. [37], and proton data at 795 MeV are from Ref. [44] and at 1200 MeV from Ref. [45]. The data are in good agreement with the expected sum curve, even at low momentum transfers, with $k_F = 236\,\mathrm{MeV}/c$ [14].

SCX sum rules for a copper sample are shown in Fig. 9 for the negative pion data of Ref. [37] at two beam energies. Uncertainties are large, but these sums are

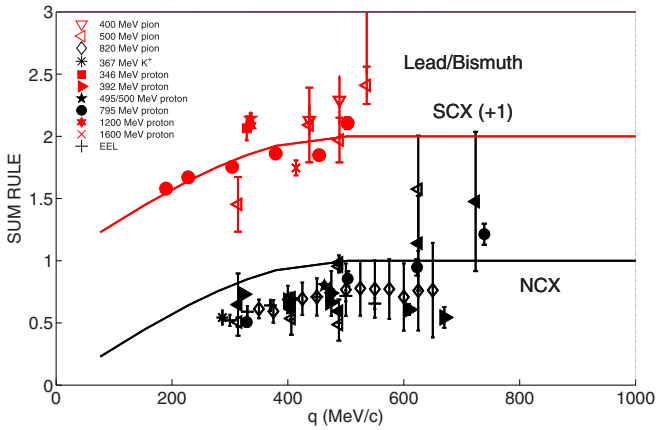


FIG. 7. As Fig. 2, but for lead and bismuth samples, with $k_F = 248\,\mathrm{MeV}/c$. Data sources are presented in the text.

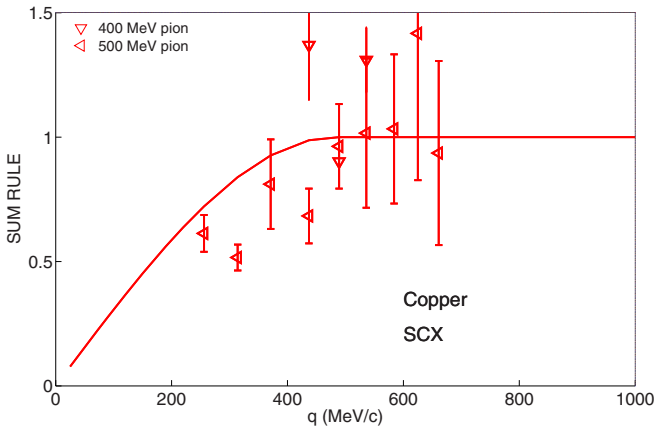


FIG. 9. As Fig. 2, but for a copper sample only for SCX spectra, with $k_F = 241$ MeV/$c$. The data are from Ref. [37].

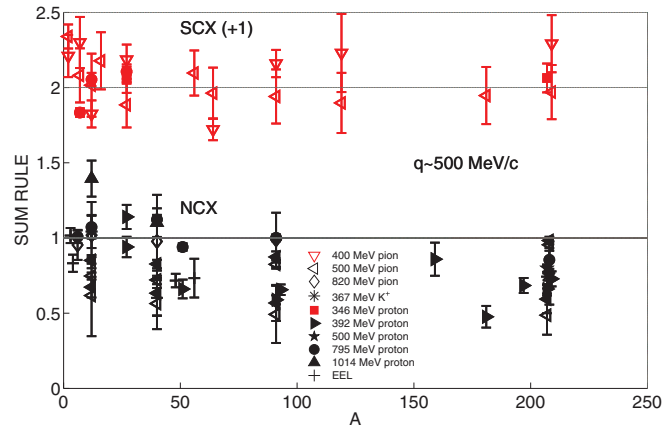


FIG. 10. Sums extracted from hadron quasifree spectra with momentum transfers $q$ near 500 MeV/$c$ presented as the target mass $A$ increases. The data sources are the same as noted in the preceding figures. Bottom, NCX results, and top, SCX results, incremented by one, in red. The 70% factor for free-space hadron-nucleon total cross sections in the Glauber model is used for this figure. Coulomb sums are included among the NCX results. The simplest expectation for these sums would be unity. The $^{3,4}$He Coulomb sums are from Ref. [4].

near agreement with the Fermi gas expectations shown for $k_F = 241$ MeV/$c$ [14].

Figure 6 shows pion SCX sum rules for zirconium [37] and a single proton point at 1200 MeV [45]. The 795 MeV SCX proton sums use the spectra of Ref. [44]. Good agreement is found with the Pauli blocking curve using $k_F = 245$ MeV/$c$ [14].

Figure 7 shows pion SCX sums from the 400 and 500 MeV $\pi^-$ spectra of Ref. [37] on bismuth. Proton SCX sums on lead at 346 MeV are from Ref. [38], at 495 MeV from Ref. [41], at 795 MeV from Refs. [43,44], and at 1200 and 1600 MeV from Ref. [45]. The nonrelativistic Fermi gas Pauli blocking curve uses $k_F = 248$ MeV/$c$ [14]. A wide range of sums is noted, scattered on both sides of the expectation.

## V. CONCLUSIONS

The fitted areas of quasifree hadron scattering spectra, expressed as sum rules, are very similar to the sum rules found for charge scattering of electrons, also shown (labeled as EEL and EET) in the figures for a wide range of nuclear samples. The $^6$Li target has half the density of carbon and heavier nuclei, and the range of hadron-nucleon total cross sections and nuclear sizes spans a wide range of nuclear densities. The hadronic spectra cover a range of momentum transfers, including the range where Pauli blocking is anticipated in the Fermi gas model. The momentum transfers for the hadrons reach as far in $q$ as do the corresponding electron scattering Coulomb sums. At higher momentum transfers pion production can be anticipated to contribute backgrounds under the inclusive hadron spectra (perhaps included in the background subtraction method used here), and the Glauber method for $A_{\rm eff}$ becomes suspect at larger angles.

These hadronic NCX data, expressed as sum rules, indicate that no major changes to strongly interacting particles or their interactions within nuclei have been sensed, as judged by the consistency with Coulomb charge sums. Moreover, the consistency of these results is evidence that the Glauber method as used has provided appropriate counts of the number of one-and-only-one collisions of the hadron beams with bound nucleons. Corresponding sums for hadronic SCX reactions suffer from poor energy resolution and a larger contribution from isovector pion production. These SCX sums show more scatter with larger error bars than do the NCX data shown in this work and rise at large angles, but offer much the same conclusions.

Figure 10 summarizes the sum rules for both NCX and SCX spectra with $q$ near 500 MeV/$c$, beyond the Pauli blocking effect. These data points have been extracted from the citations for the previous figures, including Coulomb sums shown as EEL. Each of the experiments giving the cross sections shown had a systematic uncertainty near 10%, not shown in the data points of Fig. 10.

Coulomb sums have been computed in several models [26,47,48], and transverse electron scattering sums were computed in Ref. [26]. The contributions of the one-body currents to both sums for carbon are shown as dashed curves in Fig. 3; these are very similar to the expectations of the Fermi gas. Two-body currents are very important for transverse electron scattering [26] but not for hadrons. Barbaro *et al.* [49] found that Coulomb sums depend somewhat upon the nucleon effective mass, which might be expected to be smaller than $M$ in the nuclear interior reached by electrons, and near $M$ in the surface reached by hadrons.

A new restatement of hadron quasifree scattering was presented as sum rules for a closer comparison to Coulomb sums from electron scattering. The range of momentum transfers is larger for the hadron data, especially for charge exchange. This enables comparison to the nonrelativistic Fermi gas and to more sophisticated models of nucleon momentum distributions. The hadron sums scatter, but overall are below the unit sum rule for NCX, as also noted for electrons, and near unity for SCX, using the 70% reduction factor from free-space total cross sections in the Glauber model. If the full free-space hadron-nucleon total cross sections had been used,

the sum rules would be increased by factors of about 1.45–1.65. This option also highlights the goal of understanding hadron-nucleon interactions within the nuclear medium.

This sum rule analysis using the 70% factor finds that no significant differences from the conclusions derived from quasifree electron scattering from nucleons within nuclei are found with hadron beams. The role of the in-medium hadron-nucleon total cross sections remains to be addressed with more careful methods, for instance, the distorted wave impulse approximation [23].


[1] M. L. Goldberger and K. M. Watson, *Collision Theory* (John Wiley, New York,1964).
[2] M. N. Rosenbluth, Phys. Rev. **79**, 615 (1950).
[3] P. Barreau *et al.*, Nucl. Phys. A **402**, 515 (1983).
[4] A. Zghiche *et al.*, Nucl. Phys. A **572**, 513 (1994).
[5] J. Jourdan, Nucl. Phys. A **603**, 117 (1996).
[6] C. F. Williamson *et al.*, Phys. Rev. C **56**, 3152 (1997).
[7] J. Morgenstern and Z.-E. Meziani, Phys. Lett. B **515**, 269 (2001).
[8] Y. Fujii *et al.*, Phys. Rev. C **64**, 034608 (2001); Y. Fujii, Ph.D. thesis, Tohoku University, 1998.
[9] D. B. Day, J. S. McCarthy, T. W. Donnelly, and I. Sick, Annu. Rev. Nucl. Part. Sci. **40**, 357 (1990).
[10] R. J. Peterson *et al.*, Phys. Rev. C **65**, 054601 (2002).
[11] R. J. Peterson, Phys. Rev. C **85**, 064616 (2012).
[12] R. J. Peterson, Nucl. Phys. A **920**, 20 (2013).
[13] J. Wise *et al.*, Phys. Rev. C **48**, 1840 (1993).
[14] C. Maieron *et al.*, Phys. Rev. C **65**, 025502 (2002).
[15] http//gwdac.phys.gwu.edu.
[16] T. W. Donnelly and I. Sick, Phys. Rev. C **60**, 065502 (1999).
[17] R. J. Glauber, in *Lectures in Theoretical Physics*, Vol. 1, edited by W. J. Brittin and L. G. Dunham (Wiley, New York, 1959), p. 315.
[18] J. Ouyang, S. Hoibraten, and R. J. Peterson, Phys. Rev. C **47**, 2809 (1993).
[19] J. D. Patterson and R. J. Peterson, Nucl. Phys. A **717**, 235 (2003).
[20] L. Ray, Phys. Rev. C **20**, 1857 (1979).
[21] C. Fuchs, A. Faessler, and M. El-Shabshiry, Phys. Rev. C **64**, 024003 (2001).
[22] R. J. Peterson, Nucl. Phys. A **740**, 119 (2004).
[23] T. Aumann, C. A. Bertulani, and J. Ryckebusch, Phys. Rev. C **88**, 064610 (2013).
[24] R. E. Chrien *et al.*, Phys. Rev. C **21**, 1014 (1980).
[25] V. N. Baturin *et al.*, Nucl. Phys. A **736**, 283 (2004).
[26] A. Lovato *et al.*, Phys. Rev. Lett. **111**, 092501 (2013).
[27] C. M. Kormanyos *et al.*, Phys. Rev. C **51**, 669 (1995); C. M. Kormanyos, Ph.D. thesis, University of Colorado Boulder, 1994.
[28] J. D. Zumbro *et al.*, Phys. Rev. Lett. **71**, 1796 (1993).
[29] T. Kin *et al.*, Phys. Rev. C **72**, 024003 (2005).
[30] H. Otsu, Ph.D. thesis, University of Tokyo, 1995.
[31] D. M. Corley *et al.*, Nucl. Phys. A **184**, 437 (1972).
[32] A. A. Cowley *et al.*, Phys. Rev. C **62**, 064604 (2000).
[33] C. Chan *et al.*, Nucl. Phys. A **510**, 713 (1990).
[34] X. Y. Chen *et al.*, Nucl. Phys. A **505**, 670 (1989).
[35] O. V. Miklukho (private communication); O. V. Miklukho *et al.*, Phys. At. Nucl. **76**, 871 (2013).
[36] H. Iwamoto *et al.*, Phys. Rev. C **82**, 034604 (2010).
[37] J. Ouyang, Ph.D. thesis, University of Colorado Boulder, 1992; Los Alamos Report No. LA-12457-T, 1992 (unpublished).
[38] T. Wakasa *et al.*, Phys. Rev. C **59**, 3177 (1999).
[39] T. Wakasa *et al.*, Phys. Rev. C **65**, 034615 (2002).
[40] T. Wakasa *et al.*, Phys. Rev. C **69**, 054609 (2004).
[41] B. Luther, Ph.D. thesis, Ohio State University, 1993.
[42] J. B. McClelland *et al.*, Phys. Rev. Lett. **69**, 582 (1992).
[43] D. L. Prout *et al.*, Phys. Rev. C **52**, 228 (1995).
[44] D. L. Prout, Ph.D. thesis, University of Colorado Boulder, 1992.
[45] S. Leray *et al.*, Phys. Rev. C **65**, 044621 (2002).
[46] J. Bystricky, F. Lehar, and P. Winternitz, J. Phys. **39**, 1 (1978).
[47] K. S. Kim, B. G. Yu, and M. K. Cheong, Phys. Rev. C **74**, 067601 (2006).
[48] I. C. Cloet, W. Bentz, and A. W. Thomas, Phys. Rev. Lett. **116**, 032701 (2016).
[49] M. B. Barbaro, R. Cenni, A. DePace, T. W. Donnelly, and A. Molinari, Nucl. Phys. A **643**, 137 (1998).